CHROM. 9136

IONS AND ELECTRONS IN THE ELECTRON CAPTURE DETECTOR

QUANTITATIVE IDENTIFICATION BY ATMOSPHERIC PRESSURE IONIZATION MASS SPECTROMETRY

M. W. SIEGEL* and M. C. McKEOWN

Extranuclear Laboratories, Inc., Pittsburgh, Pa. 15238 (U.S.A.)

SUMMARY

The atmospheric pressure ionizer (API) for mass spectrometry (MS) is essentially an electron capture detector (ECD) in which negative and positive ion densities are measured instead of electron density. In API–MS the ECD exhaust gas with ions entrained enters a vacuum chamber equipped to focus and mass analyze ions. When ECD response is saturated, negative and positive ion densities are equal. With cleanup, negative ions disappear but positive ion density changes only slightly. Inclusion of space charge dynamics in ECD theory resolves the discrepancy between the starting assumptions in many ECD models and the observations described. The mass spectral information of API–MS further aids modeling of ECD response.

INTRODUCTION

The electron capture detector (ECD)[1,2] remains, after nearly twenty years of practical development and theoretical analysis, a device whose response is related to the size and nature of the sample more by calibration than by calculation. The observed average electron density is determined by the interaction of time-dependent functions describing the electron production mechanism, the neutral species present, the numerous species of positive and negative ions, and by the details of the measurement technique itself. Terminal equilibrium states of ion-molecule and electron-molecule reactions are observed, so the detector response depends not only on the sample and carrier gas identities but significantly on the trace-level contaminants in each. Despite this potentially delicate dependence on details, there is little observational information about the actual ion identity in even the cleanest ECD devices.

The atmospheric pressure ionizer (API)[3,4], a newly developing ion source for high-sensitivity mass spectrometry (MS), is in its mechanical realization an obvious descendent of the ECD, on which its design is based; indeed, it is easy to visualize a single device operable in either ECD or API–MS modes. The contrasting new re-

---

* To whom correspondence should be addressed. Full address: Extranuclear Laboratories, Inc., P.O. Box 11512, Pittsburgh, Pa. 15238, U.S.A.

quirement for API is that the ECD gas outlet be a gas and ion sampling aperture into the MS vacuum system. With moderately fast vacuum pumps, the entire gas flow typical of ECD operation can be accomodated to a pressure suitable for operation of the MS. Additional requirements for the API–MS are external to the ionization region. They consist of electrostatic lenses in the vacuum to separate ions from the gas jet and focus them into the entrance aperture of the MS, and appropriate electrical circuitry to bias the MS for selection and detection of positive or negative mass analyzed ions. From the point of view of the ECD user, the API–MS is an ECD fully instrumented so that its macroscopic current response can be correlated with the microscopic details of the positive ion, negative ion and free electron densities.

APPARATUS

To give the reader a clear picture of how the API ion source and the associated MS system can be compared to an ECD and its associated instrumentation we begin with a description of the apparatus.

API source
The source described is designed for direct injection of microlitre liquid sample aliquots without chromatographic preseparation. Inspection of the simplified drawing (Fig. 1) shows that introduction of GC effluent in place of liquid samples should be straightforward. Important design features include: (1) The active volume is electrically isolated, so its potential can be established for interfacing to the mass spectrometer. (2) Materials and construction techniques are compatible with operation and bakeout temperatures in the 200–400° range. (3) Gas flow paths are designed so as to maximize the fraction of sample delivered to the active volume and vacuum system while residual flashback material is continuously flushed away from the active region. (4) The device can be easily removed for cleaning, aperture replacement, etc.
With the addition of a collection electrode, for example an axial pin[2], the API could clearly be operated as an ECD by monitoring the average electron density. Alternatively, the total negative ion current emerging from the aperture can be measured, giving a signal complementary to the usual ECD signal.

Vacuum system
To maximize system sensitivity all the carrier gas ($0.1–1.0$ atm ml sec^{-1}) should enter the vacuum system. A pumping speed of the order of 1000 l sec^{-1} is required to maintain a pressure sufficiently low that ions can be electrostatically separated from the gas jet and focussed into the mass analyzer without serious scattering losses ($\leqslant ca.\ 3 \times 10^{-4}$ torr). The appropriate aperture diameter is typically 25–50 μm. The mass analyzer and particle multiplier require a still lower pressure, a few times 10^{-5} torr at most, and preferably of the order of 10^{-6} torr. A differentially pumped system is most appropriate, maintaining approximately 3×10^{-4} torr in the low-pressure focus chamber and approximately 1×10^{-6} torr in the mass analysis chamber. We use two 800 l sec^{-1} turbomolecular pumps in our apparatus (Airco Temescal Model TMP 814). To minimize scattering and optical losses, the distance from the ion source aperture to the mass analyzer entrance aperture should be no more than 5–10 cm, the distance required to clear gas dynamic effects and physically accomodate
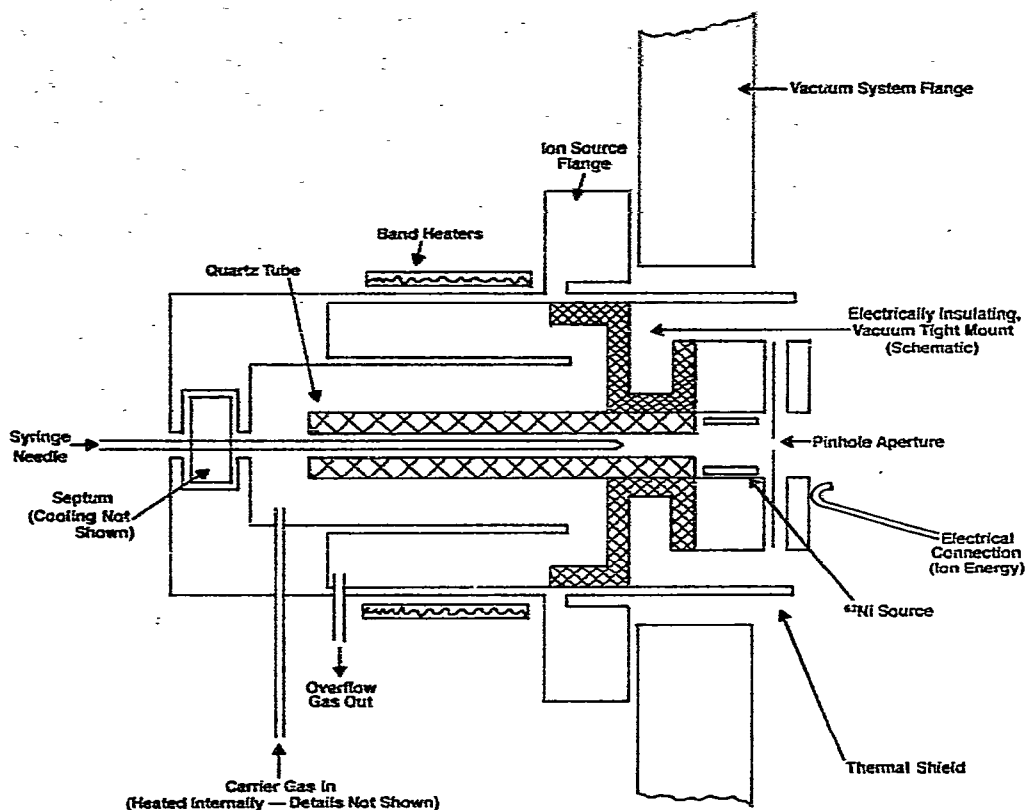
Fig. 1. Schematic diagram of API ion source.

the low-pressure optics. Since the pumps have a 42.5-cm throat diameter, the mass analysis chamber is constructed with a "top hat" deeply re-entrant into the low-pressure focus chamber.

Ion focus–mass analyzer–signal system

Ions diverge from the API source aperture entrained in the gas flow for a few millimeters, until the gas density is sufficiently low that electrostatic lens forces can dominate their motion. A four-element lens (partly constructed of mesh for transparency to gas flow) is used to refocus these ions into the mass analyzer entrance aperture. A filament attached to the lenses can act as an occasional electron source providing an electron impact spectrum during mass calibration.

Mass analysis is by a quadrupole mass filter equipped with a particle multiplier detector and ion-counting electronics (Extranuclear Labs, spectrEL, modified). The operating background level of the detection system is less than 5 counts sec^{-1}, and the counting-type particle multiplier is usable to about 10^6 counts sec^{-1}. Typical count rates on large reactant ion peaks (e.g., $H_3O^+ \cdot H_2O$) approach 10^5 counts sec^{-1} at better than unit resolution. Data are accumulated by a multiple ion detection (MID)[5] technique using four single-channel scalers or by similar techniques with the instru-

ment under software control by a minicomputer, or by a ratemeter and oscilloscope or chart recorder display for broad mass scans.

ION DENSITY, ELECTRON DENSITY AND ION CURRENT

In this discussion positive ion, negative ion, and electron densities and currents will be evaluated in several limiting cases and in general. The notation is as follows: (1) All densities are symbolized by n. (2) n^0 refers to densities in the quiescent, *i.e.*, clean, no-sample, state. (3) n^∞ refers to densities in the saturated, *i.e.*, very-large-sample state. (4) n without a superscript refers to intermediate states. (5) n_e, n_+ and n_-, with or without superscript, always refer to electron, positive ion and negative ion densities, respectively. (6) $n_\pm$ is used to symbolize equal charge densities of each sign. Thus $n_\pm^0$ symbolizes equal quiescent values of positive ion and electron density, $n_\pm^\infty$ symbolizes equal saturation values of positive ion and negative ion densities, and $n_\pm$ without superscript symbolizes a positive ion density equal to the sum of negative ion and electron densities.

It is generally assumed in the ECD literature that in the quiescent state the carrier gas and detector body are sufficiently free of gas phase electronegative molecules that the negative charge resides almost entirely in a thermal electron cloud. Given this assumption and the physical parameters of the device, it is straightforward to estimate the charge densities. At equilibrium the ion–electron pair production rate due to primary electrons (^{63}Ni β-rays) is balanced by three loss mechanisms: flow loss carried by the gas stream, wall loss due to diffusion, and recombination loss between positive ions and thermal electrons. For a 1-mCi ^{63}Ni primary source with good geometry the ion–electron pair production rate, S, is about 1.8×10^{10} sec^{-1}, assuming 17keV average primary energy* and one pair per 35eV primary energy[7]. Flow loss and diffusion loss rates are linear in the respective ion and electron densities, and the recombination loss rate depends on the product of these two densities.

Taking the usual assumption that the electron and positive ion clouds diffuse independently, for the clean quiescent detector the relevant rate equations are:

$$S = F n_e^0 + k D_e n_e^0 + R_0 V n_e^0 n_+^0 \tag{1a}$$

$$S = F n_+^0 + k D_+ n_+^0 + R_0 V n_\pm^0 n_e^0 \tag{1b}$$

where F is the gas flow-rate (approximately 0.3 ml sec^{-1}), D_+ and D_e are the diffusion constants for positive ions and electrons (approximately 0.05 and 50 cm^2 sec^{-1}, respectively, at 1 atm[8], R_0 is the ion–electron recombination rate (approximately 3×10^{-6} ml sec^{-1})[9], k is a geometrical constant determined by the radius and the length of the active volume ($k \approx 16$ cm for 0.25 cm length and 0.3 cm radius)[10], and V is the source volume (approximately 0.1 ml). Substituting these values into eqns. 1a and 1b gives $n_+^0 \approx 5.6 \times 10^9$ ml^{-1} and $n_e^0 \approx 7.4 \times 10^6$ ml^{-1}, the smaller electron density being due to the assumed more rapid electron diffusion to the walls.

This conventional treatment, which yields the familiar result that the positive

---

* The maximum β-ray energy is 65.9 keV, the average being considerably less because the total nuclear transition energy is shared between the β-ray and a neutrino. See, *e.g.*, ref. 6.

ion density far exceeds even the quiescent (or clean) electron density in an ECD, neglects an important space charge effect which couples the electron and positive ion diffusion rates. When charge densities exceed approximately 10^7 ml^{-1}, the negative and positive charge clouds begin to interact sufficiently strongly that the contents of the active volume must be treated as a plasma, with local charge neutrality being the rule. The space charge interaction causes the electron diffusion rate to be strongly decreased, and the ion diffusion rate to be slightly increased, such that both electrons and positive ions become characterized by a single (ambipolar) diffusion coefficient[11].

$$D_a = \frac{D_+ K_e + D_e K_+}{K_e + K_+} \tag{2}$$

where K_+ and K_e are the respective mobilities in an electric field (cm^{2}sec^{-1} V^{-1}). It is easily shown that when ions, electrons and neutrals are all characterized by the same temperature, $D_a \approx 2 D_+$. Eqns. 1a and 1b then reduce to one equation for the single valued charge density $n_\pm \equiv n_+ = n_e$

$$S = F n_\pm^0 + k D_a n_\pm^0 + R_0 V n_\pm^{0^2} \tag{3}$$

The solution gives $n_\pm \approx 2.4 \times 10^8$ ml^{-1}.

Typical numbers are of a size such that flow and diffusion losses have only a small effect compared to the dominant recombination processes, so

$$n_\pm^0 \approx \left(\frac{S}{R_0 V}\right)^{\pm} \tag{4}$$

We now consider the case of an ECD–API saturated by a large sample density. The above arguments about dynamical space charge effects remain applicable. We expect, and find experimentally, that in the API with a high concentration of electron capturing impurities the positive and negative ion densities are equal and the electron density is so small as to be undetectable by normal ECD instrumentation. The equal positive and negative ion densities during saturation, $n_+^\infty = n_-^\infty \equiv n_\pm^\infty$, are determined by

$$S = F n_\pm^\infty + k D_\pm n_\pm^\infty + N_0 Q V n_\pm^{\infty^2} \tag{5}$$

where we have set $D_+ = D_- \equiv D_\pm$, where Q is the rate constant for three-body recombination of positive and negative ions mediated by the carrier gas, and where N_0 is the carrier gas density. Typical values of Q are of the order of 2×10^{-25} ml^2 sec^{-1} [12], and N_0 is approximately 2.5×10^{19} ml^{-1}, so the product $N_0 Q$ in eqn. 5 is of the same order of magnitude as R_0 in eqn. 1b. It thus follows that in the saturated response case

$$n_\pm^\infty = \left(\frac{R_0}{N_0 Q}\right)^{\pm} n_\pm^0 \tag{6}$$

Since the coefficient of $n_\pm$ in eqn. 6 is near unity, only small changes in charged particle density accompany the introduction of even larger samples.

In the general case where it is necessary to include positive ion, negative ion and electron densities, there are three coupled rate equations

$$\frac{dn_+}{dt} = \frac{S}{V} - R_0 \, n_e \, n_+ - R_2 \, n_- \, n_+ \tag{7a}$$

$$\frac{dn_e}{dt} = \frac{S}{V} - R_1 \, (n_A - n_-) \, n_e - R_0 \, n_e \, n_+ \tag{7b}$$

$$\frac{dn_-}{dt} = R_1 \, n_e \, (n_A - n_-) - R_2 \, n_+ \, n_- \tag{7c}$$

Here R_2 is the phenomenological rate constant for negative ion–positive ion recombination (explicitly denoted $N_0 Q$ above), and R_1 is the electron attachment rate constant for sample molecules of type A. n_A is the sample density of A in the carrier gas stream before it reaches the reaction volume where the sample molecule density is less than n_A due to sample depletion by negative ion formation. For simplicity diffusion and flow losses have been omitted, since their effect is easily shown to be small in normal circumstances. It is implicit in these rate equations that $n_+ = n_e + n_-$.

At equilibrium each derivative is zero. In the no-sample and saturating-sample regimes these equations effectively reduce to eqns. 4 and 6, respectively. In the intermediate regime where the negative charge cloud contains significant electron and negative ion densities numerical techniques are required to obtain a solution. However, in the quasi-linear regime characteristic of small samples, where $n_- \ll n_e$, i.e., the practical ECD operation regime, it is easily shown that as a first approximation

$$n_+ \approx n_+^0 \tag{8a}$$

$$n_e \approx n_e^0 \tag{8b}$$

$$n_- \approx \frac{R_1}{R_2} \, n_A \ll n_e \tag{8c}$$

Reimposing the requirement of total charge neutrality yields, as a second approximation to the electron density

$$n_e \approx n_e^0 - n_- \tag{9a}$$

$$n_e \approx \left(\frac{S}{R_0 V} \right)^{\pm} - \frac{R_1}{R_2} \, n_A \tag{9b}$$

n_e being the primary signal in ECD, that is, before backing-off is imposed. An interesting point revealed by these equations appears to be inadequately emphasized in

the ECD literature. n_e clearly depends on the radioactive source strength S. But when the standing current, proportional to n_e^0, is backed-off any change in electron density due to a change in sample concentration is equal to the change in n_- and is independent of S.

We would also like to expand on our conclusion via eqn. 6 that the magnitude of the charged particle density in an ECD or API is relatively constant and independent of whether or not electron capturing species are present in excess. This statement hinges on our assertion that positive ion–negative ion recombination rates at atmospheric pressure are typically of the same order of magnitude as positive ion–electron recombination rates. The size of these rate constants is well established for simple species of atmospheric interest, and the literature strongly supports us in stating that in these cases R_0 and R_2 are quite comparable[13]. In contrast, it has become entrenched in the ECD literature that R_2 exceeds R_0 by five to eight orders of magnitude [see refs. 14 (especially pp. 163 and 171) and 15]. We feel certain that even for complex organic molecules this is not possible. The reaction cross-sections are almost entirely determined by the very strong coulomb interaction between oppositely charged particles, and the geometrical factors due to molecular size can only slightly increase the rate constants for large organic molecules over simple species. Since the ratio of charged particle densities in quiescent and saturated cases is determined by the square root of the ratio of the corresponding recombination rates, even in the most extreme cases we can envision there would be less than an order of magnitude change in charge density when passing from quiescent to saturated states.

For completeness we add that at large but incompletely saturating sample levels the total electron density is inversely proportional to the sample concentration in the carrier gas stream

$$n_e \approx \frac{S}{R_1 \, n_A \, V} \tag{10a}$$

and

$$n_+ \approx n_- \approx \left(\frac{S}{R_2 V} \right)^{\pm} \tag{10b}$$

We are now able to compare the signals obtained in ECD and API–MS for a given sample density n_A. In the ECD with standing current backed off, a measurement of the electron density yields a difference current

$$I = -C \, e \, n_- \, V \tag{11a}$$

$$I = -C \, e \, \frac{R_1}{R_2} \, n_A \, V \tag{11b}$$

where e is the electron charge and C is a constant describing the sampling process. In the pulsed mode C is equal to the pulse rate in Hz if each pulse clears the active volume of electrons and the pulses are sufficiently infrequent that equilibrium is restored between them.

In API–MS the total ion and electron currents into the mass spectrometer vacuum should be the products of gas flow-rate with the corresponding charge densities

$$I_+ = e\,F\,n_+ \approx e\,F\,n_+^0 \approx +1.2 \times 10^{-11}\,\mathrm{A} \tag{12a}$$

$$I_e = e\,F\,n_e \approx \begin{cases} e\,F\,n_e^0 \approx -1.2 \times 10^{-11}\,\mathrm{A} & \text{for small samples} \quad\ (12b) \\ 0 & \text{at saturation} \qquad\quad\ (12c) \end{cases}$$

$$I_- = e\,F\,n_- \approx \begin{cases} e\,F\,\dfrac{R_1}{R_2}\,n_\mathrm{A} & \ll I_e \text{ for small samples} \quad (12d) \\[2mm] -e\,F\,n_+^\infty \approx -1.2 \times 10^{-11}\,\mathrm{A} \text{ at saturation} \quad (12e) \end{cases}$$

The change in ECD current (eqn. 11b) is clearly equivalent to the API negative ion current (eqn. 12d).

An experimental check of the ion density calculations has been made by absolute current measurements using apparatus such as is depicted in Fig. 2. The measured positive ion current or negative ion current at saturation is about 0.5×10^{-11} A, about 40% of the calculated value. Given the idealizations invoked in the calculation, we consider the agreement quite reasonable.

The measured electron current is much smaller than the value of I_e given by eqn. 12b. This is because charge density equality (ambipolar diffusion) is the rule only at distances greater than one Debye length from a boundary surface, in this case about 50 μm[16]. Since the aperture diameter and thickness are comparable to the Debye length, the electrons in the aperture are lost by diffusion at about 1000 times the rate positive and negative ions are lost.

Finally, we point out that the noise on the ECD current is determined by the statistical fluctuations associated with the standing current. Backing off the standing current does not reduce this noise and in fact somewhat worsens the measurement noise. These fluctuations set the limit on ultimate sensitivity (smallest detectable sample density). In contrast an API–MS system measures the negative ion density directly. Its ultimate sensitivity is set by the background counting rate of the ion counting system, and therefore should considerably exceed that of ECD detection. This conclusion appears to be confirmed experimentally (refs. 4 and 17 and references in ref. 17).

THE QUIESCENT SPECTRUM

The ECD is assumed to be clean and ready for use when after some bakeout period no further increase in electron current is observed. This criterion does not guarantee that electron capturing species have been eliminated, only that their concentration in the detector has reached an equilibrium level. In contrast, with API–MS we can observe the disappearance of the negative ion spectrum as the source cleans up: when the negative ions are gone, the source is clean.

To ensure cleanliness, materials and procedures similar to those used in GC–ECD work are employed. The API itself is of all metal, quartz and ceramic construction. Multiple gas flow paths within the API provide for continual flushing of the ce-
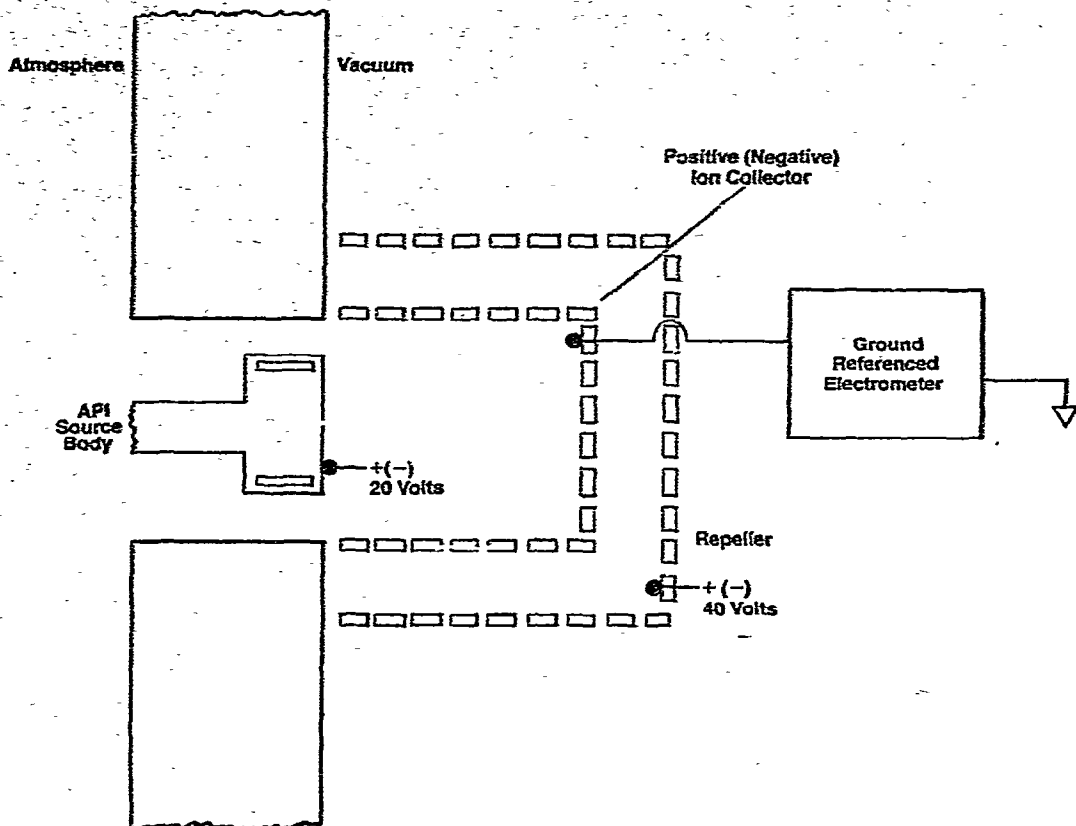
Fig. 2. Schematic diagram of apparatus used to measure total charge (of either sign) from API ion source into vacuum chamber.
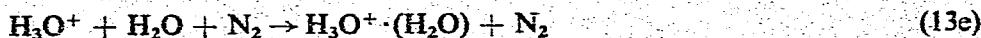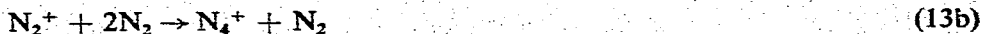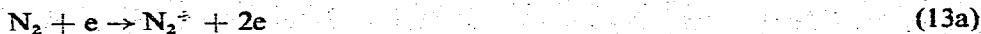
ramic parts, so migration of retained impurities from ceramic surface irregularities into the active volume is eliminated. Materials, construction techniques, and cleaning procedures identical to those used on ultra-high vacuum components are employed. The API parts are then subjected to a "supercleaning" and silanization procedure including ultrasonic treatment with hot KOH in methanol, appropriate rinsing, ultrasonic treatment with hot dichlorodimethylsilane in toluene, appropriate rinsing, predrying for 1 h in clean flowing nitrogen at 80°, and an overnight bake in clean flowing nitrogen at 400°. The carrier gas used is ultra-pure nitrogen or the boiloff from sealed liquid nitrogen dewars; even with these precautions an occasional tank must be rejected. Gas pressure regulators are of the ultra-high purity type, with welded stainless-steel diaphragms. The gas is filtered through a stainless-steel trap filled with 13X molecular sieve, followed by a stainless-steel particle filter. The trap and filter are baked every night at about 300° with gas flowing. Ultra-fine metering valves of all welded stainless-steel construction are employed for flow control. All gas lines are stainless steel, and all connections are made with stainless-steel Swagelok™ fittings. Upon installation and from time to time thereafter the gas lines and fittings are flamed to a cherry red color with a vigorous gas flow, moving from tank to API source. The

API source is actually operated at slightly above atmospheric pressure, which provides dynamical sealing and allows convenient regulation of internal pressure (rather than flow-rate) by means of a long overflow tube terminated about 5 cm under water.

When a source is first installed it is invariably the case that no matter how scrupulous previous chemical scrubbing has been, negative and positive ion spectra are so dense with mass peaks as to be nearly uninterpretable; the uniform feature is that total negative ion current is equal to total positive ion current, and the magnitude of the total currents is nearly independent of the spectral details. If the chemical scrubbing has been adequate, then after about 1 h at 400° the positive ion spectrum will be dominated by $H_3O^+ \cdot (H_2O)_n$ and the negative ion spectrum will be dominated by $Cl^- \cdot (H_2O)_n$ and frequently $O_2^- \cdot (N_2)_n$; the total negative ion current will still equal the total positive ion current. After another hour, the negative ion spectrum will usually contain only Cl^-, sometimes with some O_2^-. Thereafter the Cl^- ion current will begin to decrease, falling essentially to zero after about 12 h baking at 400°. There is occasionally a small residual O_2^- peak, usually traceable to carrier gas contamination. The total positive ion current usually drops 20–50% from its initial value (see eqn. 5). If the chemical scrubbing has been faulty, copious negative ion currents may be seen for several days. If after cleanup the source has to be rapidly cooled, removed as for blowing out a clogged aperture and replaced, with only a 10-min exposure to air, *in situ* cleanup is again required but takes about 1 h instead of 12 h. Our pre-cleaning procedure and our choice of materials appear to be at least as good as those employed in normal GC–ECD work. The impressive time which must then be devoted to *in situ* high temperature baking to eliminate residual negative ions leads us to question whether very many of the ECDs in current use are ever truly clean enough to have electrons as the only negative charge carriers. This question may be particularly pertinent to ECDs using tritium in occluded form as the active foil.

When the API source is clean and negative ions have been eliminated, the striking feature of the quiescent positive ion spectrum is the extent to which it is dominated by minute traces of water vapor in the carrier gas. It might normally be expected that with a nitrogen carrier the dominant spectrum would be $N_2^+ \cdot (N_2)_n$, and, to a lesser extent, $N^+ \cdot (N_2)_n$. These ions have indeed been seen in an API using a corona discharge (where the ions can be produced in close physical proximity to the vacuum aperture) but with ^{63}Ni sources the dominant ions are $H_3O^+ \cdot (H_2O)_n \cdot (N_2)_m$.

The formation route for $H_3O^+ \cdot (H_2O)_n$ has been proposed as

$$N_2 + e \rightarrow N_2^+ + 2e \tag{13a}$$

$$N_2^+ + 2N_2 \rightarrow N_4^+ + N_2 \tag{13b}$$

$$N_4^+ + H_2O \rightarrow H_2O^+ + 2N_2 \tag{13c}$$

$$H_2O^+ + H_2O \rightarrow H_3O^+ + OH \cdot \tag{13d}$$

$$H_3O^+ + H_2O + N_2 \rightarrow H_3O^+ \cdot (H_2O) + N_2 \tag{13e}$$

It is not yet entirely clear whether this scheme is consistent with our observations. A good understanding of the formation route of the quiescent state spectrum is re-
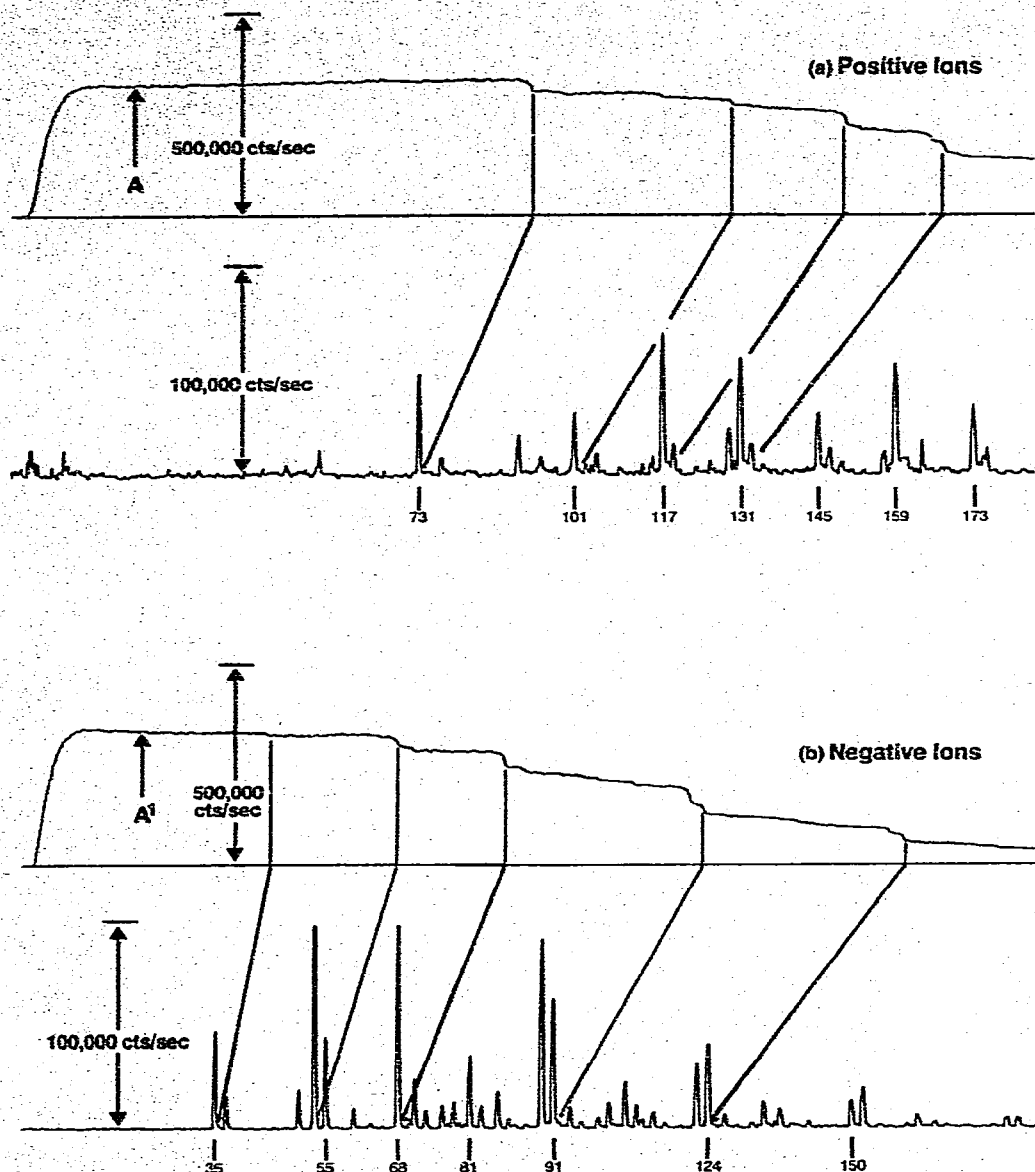
Fig. 3. (a) Positive ion spectrum of newly installed API ion source, before *in situ* baking. The upper trace is an integral spectrum (amplitude at any mass number represents total of all heavier ions), the lower trace is a normally resolved spectrum. The mass scale in the integral spectrum is stretched by a factor of 9/7. (b) A negative ion spectrum simultaneous with 3a. Comparison of counting rates below the lowest resolved mass (*e.g.*, points A and A') shows the equality of positive and negative ion densities.

quired because response to a sample may be dominated not by interactions with $H_3O^+ \cdot (H_2O)_n \cdot (N_2)_m$, but by interactions with intermediate ions never observed in the quiescent state. This is of relevance to the ECD user as well as to the API user interested in positive ion detection, because in some cases the formation of negative
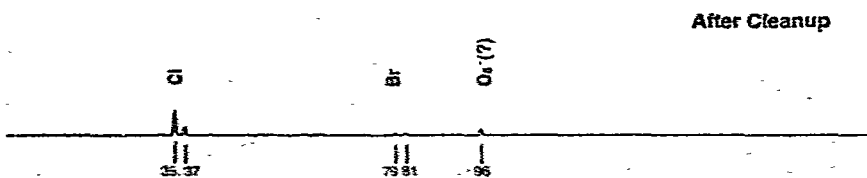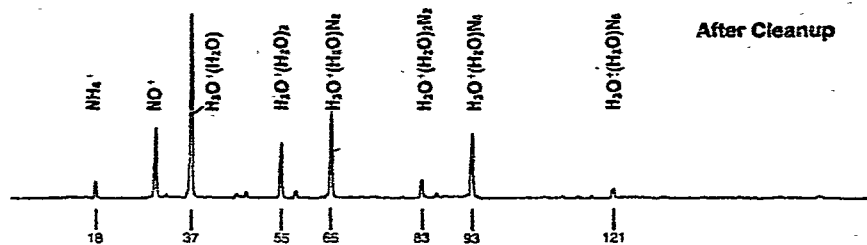
Fig. 4. (a) Positive ion spectrum approximately 1 h and approximately 12 h after installation of a freshly cleaned API ion source. (b) Negative ion spectra, simultaneous with 4a.

ions may be preceded by attack on the sample molecule by positive ions or free radicals whose presence depend on the details of the positive ion-forming impurities in the carrier gas.

Figs. 3a and 3b show the positive and negative ion spectra obtained from a chemically scrubbed but newly installed API. In each case the upper trace is an integral or total ion spectrum and the lower trace is a normally resolved spectrum. The integral spectra, examined at low mass (*e.g.*, points A and A') demonstrate the equality of positive and negative ion currents from the API.

Figs. 4a and 4b show the effect of approximately 12 h of cleanup at 400°.

Response to several illustrative samples

The response obtained from the API is complementary and supplementary to the ECD response for an equivalent sample under similar operating conditions: complementary in that measuring the total negative ion signal is equivalent to measuring the decrease in electron density, and supplementary in that positive and negative ion species are identified and quantified by the mass spectrum.

The accompanying figures show data on three sample and response types: (1) 2,3,7,8-tetrachlorodibenzo-*p*-dioxin (TCDD) observed as the parent negative ion, (2) 2,4,5-trichlorophenoxyacetic acid (2,4,5-T) observed as the trichlorophenoxide negative ion, and to demonstrate response in the positive ion mode (3) nicotine observed as the MH^+ positive ion.

In each case 1-μl benzene solution samples were introduced by syringe directly into the quartz tube leading to the reaction volume (Fig. 1). Formation of solvent positive ions modifies the positive ion spectrum, the effect this has on response in the positive ion mode having been previously discussed by other authors[18].

For the purpose of discussing the data, modification of the positive ion spectrum is of secondary importance. On the other hand, in our experience the best available benzene always contains a sufficiently high concentration of electron-attaching impurities that a negative ion spectrum (usually dominated by Cl^-) is seen even from "blank" samples. Thus were it not for mass spectral separation or chromatographic preseparation, the API would be useless as an analytical detector for samples in solution. Even with mass spectral separation, the solvent impurities compete with the sample for the nearly fixed available electron charge, and solvent purity often determines the smallest practical detectable sample. For these reasons, as well as for ease of spectral interpretation, we anticipate that the GC–API–MS combination will ultimately be used to best exploit the API method. The following data nevertheless speak for themselves in demonstrating the sensitivity and specificity of API–MS in comparison with GC–ECD.

Fig. 5 shows detector response to 250 fg of TCDD in 1 μl of benzene with two sample injections separated by a blank solvent injection. The trace is obtained by recording *vs.* time the output of a ratemeter while the mass spectrometer is set to monitor the molecular negative ion $TCDD^-$ at 322 a.m.u. (the most abundant isotope).

Fig. 6 shows a mass spectrum of the trichlorophenoxide negative ion at mass 195 and isotopes, obtained from a 2,4,5-T sample. Approximately 1 pg of 2,4,5-T is required to obtain a continuous spectrum of this quality, obtained by a signal averaging device [Princeton Applied Research (PAR) Waveform Eductor (100 channels)], while the mass range is rapidly and repetitively swept for approximately 30 sec,

Fig. 5. Response to samples of 250 fg TCDD in 1 µl benzene, separated by a blank benzene sample. The TCDD$^-$ ion is monitored.
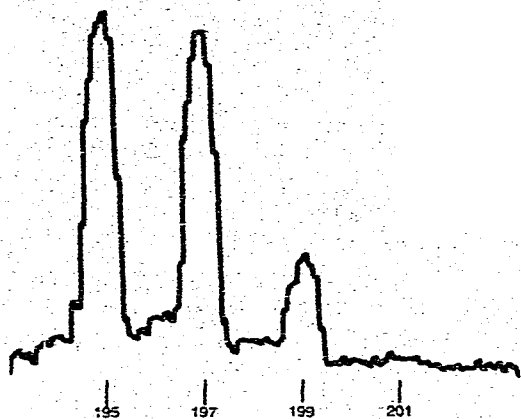

Fig. 6. Resolved spectrum of 2,4,5-T as the trichlorophenoxide negative ion at 195, 197, 199, and 201 a.m.u. A large sample (1 pg) is required to obtain a continuous spectrum, but by MID techniques 100 fg can be detected with a signal-to-noise ratio of about 3:1. The steps in the record are characteristic of the 100-channel signal averager (see text).

beginning just before sample injection. Using the multiple ion counting detection technique, a detection limit of 100 fg is attained and essentially linear response to approximately 2000 fg is observed. Data demonstrating this sensitivity and linearity have been published previously[19]. With 2,4,5-T several other ions are observed less sensitively. These include several fragments as both positive and negative ions, and a dimer negative ion.

Fig. 7 shows detector response to a series of nicotine samples, in which the protonated nicotine ion (MH$^+$) is monitored at 163 a.m.u. The limit of detectability is in this case determined by the nicotine content of the solvent, seen to be about 2 pg/µl (2 µg/l). Other ions observed in the scanning mode are singly ionized nicotyrene and protonated nicotyrene at 158 and 159 a.m.u., and singly ionized nicotine at
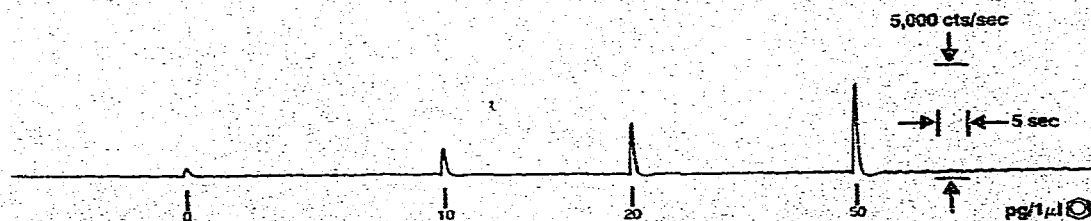

Fig. 7. Response to nicotine as the MH$^+$ ion at 163 a.m.u. The detection limit appears to be set by solvent contamination.

162 a.m.u. The unprotonated nicotine and nicotyrene peaks decay in time about five times as rapidly as the peaks corresponding to the protonated ions, indicating the existence of important but as yet not understood dynamical effects.

A compendium of various positive and negative ions observed in several API–MS configurations has been given in ref. 4.

Applications of mass spectral information to ECD theory and technology

Our previous discussion has emphasized the relevance to ECD theory and technology of the total negative and positive ion densities determined by an API instrument, and has touched only briefly on the extent to which mass spectral information might be useful. The reason is twofold:

The results of the total ion density measurements are simple, completely general, and can be immediately incorporated into new theoretical treatments and experimental interpretations. In contrast, the mass spectral observations during response to sample are often complicated by the observation of several positive and negative ion species associated with one sample type. They are specific to the relatively small number of sample types tried, and they have mainly been of large molecules, the details of whose interaction with the API–ECD plasma are at best speculative.

We can anticipate several ways in which a body of API–MS data, particularly data on the positive ion spectra of simple molecular gaseous species, will eventually aid in the optimization of ECD operation when there are specific requirements such as high sensitivity, large dynamic range, etc.

Differential sensitivity. For example, consider an application in which it is necessary to distinguish delicately between samples of nearly equal size. From eqn. 6 we see

$$\frac{dn_-}{dn_A} = \frac{R_1}{R_2} \tag{14}$$

where R_1 is the rate constant for electron attachment to sample A and R_2 is the negative ion–positive ion recombination rate. R_1 depends weakly on the nature of the carrier gas (mediating three-body attachment), but R_2 can depend strongly on the specific positive ion type present. By selecting a carrier gas, or by trace doping of the carrier, to produce positive ions having a small value of R_2 in recombination with the negative ions from A, the derivative (eqn. 14) can be made relatively large, *i.e.*, the response can be made very sensitive to small changes in n_A. To be specific, positive ion–negative ion recombination is faster when the positive ions are clustered than when they are simple[13,20], so if high differential sensitivity is required, clustered positive ions should be avoided.

Ultimate sensitivity. Unity signal-to-noise ratio in the ECD occurs at the sample density for which the captured current is equal to the statistical fluctuation current due to the standing electron density. Defining the sample density n_A^0 as the lowest detectable value of n_A, eqns. 8c and 4 give

$$n_A^0 = \frac{S^{\frac{1}{2}} R_2}{R_0^{\frac{1}{2}} R_1 V^{\frac{1}{2}}} \tag{15}$$

Thus ultimate sensitivity is also enhanced by minimizing R_2, i.e., minimizing the density of clustered positive ions. Doing so will generally also have the effect of minimizing R_0, the positive ion–electron recombination rate[13,20], but $R_0^{\frac{1}{2}}$ rather than R_0 appears in the denominator, and the denominator decreases only slightly with decreasing degree of clustering.

Dynamic range. A useful measure of the maximum usable sample density is provided by the intersection of the straight line describing negative ion density (loss of electron density) at small values of n_A, with the straight line describing electron density at large values of n_A. Denoting the value of n_A at the intersection by n_A^1, eqns. 8c and 10a give

$$n_A^1 = \frac{S^{\frac{1}{2}} R_2^{\pm}}{R_1 V^{\pm}} \tag{16}$$

The dynamic range is thus

$$\frac{n_A^1}{n_A^0} = \frac{R_0^{\pm}}{R_2^{\pm}} S^{\pm} V^{\pm} \tag{17}$$

Considerations identical to those argued in the previous case indicate that it is again desirable to minimize the degree of clustering.

It is interesting to observe that differential sensitivity, ultimate sensitivity and dynamic range in the ECD can all be controlled by small concentrations of dopants in the carrier gas affecting only the positive ion spectrum. Yet the positive ion spectrum has heretofore been entirely ignored in ECD work.

There may be a variety of considerations applicable to the detailed negative ions present in the ECD. We will illustrate with a single example.

Mechanisms of neutralizing negative ions. The residence time of a sample molecule in an ECD is typically of the order of 0.5 sec. The lifetime against electron capture for strongly attaching species is of the order of 0.05 sec. Suppose that a sample molecule attaches an electron to form the negative molecular ion and then recombines with a positive ion by mutual neutralization to regenerate the original sample molecule. (Recombination rates are larger by a factor of 10^3 than electron attachment rates and do not perturb the argument). The recycled neutral can consume the order of ten electrons during its passage through the ECD and the reduction in electron density will be registered as a strong ECD response. To enhance this effect it may be advantageous to use low gas flow-rates. By contrast, suppose that the negative ion or its recombination products undergo complex dissociation or rearrangement to produce neutrals with either zero or very small electron attachment rate coefficients. Then clearly each initial sample molecule can only remove one electron during its passage through the ECD, producing a relatively weak ECD response. A high flow-rate under these conditions would promote the entry of fresh electron attaching neutrals and consequently increase the change in the time averaged electron density. A knowledge of the negative ions produced in the ECD should allow systematic tailoring of the flow-rate and other parameters to enhance sensitivity.

CONCLUSION

API–MS has already made what we anticipate will be an important contribution to the initial assumptions going into ECD theories by demonstrating that (1) positive and negative charge densities are numerically equal in the active volume and (2) the charged particle density is relatively insensitive to whether the negative charge consists of electrons or negative ions. Furthermore it is shown that relevant ECD descriptors such as differential sensitivity, ultimate sensitivity, and dynamic range can be strongly affected by the nature of the positive ions present, and the positive ion spectra of various carrier gas mixtures can be productively studied by API–MS. The inter-relationship between negative ion dynamics and external factors such as flow-rate and temperature is pointed out, and it is shown that API–MS can be used to identify the terminal negative ions in an ECD active volume, making it possible to decide systematically the proper operating conditions for specific sample types.

ACKNOWLEDGEMENTS

REFERENCES

1 J. E. Lovelock, *J. Chromatogr.*, 99 (1974) 3.
2 A. Zlatkis and D. C. Fenimore, *Rev. Anal. Chem.*, 2, No. 4 (1975) 317.
3 E. C. Horning, M. G. Horning, D. I. Carroll, I. Dzidic and R. N. Stillwell, *Anal. Chem.*, 45 (1973) 936.
4 M. McKeown and M. W. Siegel, *Amer. Lab.*, November (1975) 88.
5 P. Irving, *Ind. Res.*, October (1974) 78.
6 J. D. McGervey, *Introduction to Modern Physics*, Academic Press, New York, 1971, p. 515.
7 D. E. Gray (Coordinating Editor), *American Institute of Physics Handbook*, McGraw-Hill, New York, 3rd ed., 1972, J. B. Marion (Editor), Section 8, Table 8d-11, p. 8-184.
8 E. W. McDaniel, *Collision Phenomena in Ionized Gases*, Wiley, New York, 1964, p. 490.
9 M. A. Biondi, in M. H. Bortner and T. Baurer (Editors) *Defence Nuclear Agency Reaction Rate Handbook*, March 1975, 4th Rev., Ch. 16, p. 16-27.
10 E. W. McDaniel, *Collision Phenomena in Ionized Gases*, Wiley, New York, 1964, p. 503.
11 E. W. McDaniel and E. A. Mason, *The Mobility and Diffusion of Ions in Gases*, Wiley, New York, 1973, p. 25.
12 M. A. Biondi, in M. H. Bortner and T. Baurer (Editors) *Dfeense Nuclear Agency Reaction Rate Handbook*, March 1975, 4th Rev., Ch. 16, p. 16-30.
13 M. A. Biondi, in M. H. Bortner and T. Baurer (Editors) *Defense Nuclear Agency Reaction Rate Handbook*, March 1975, 4th Rev., Ch. 16.
14 J. E. Lovelock, *Anal. Chem.*, 33 (1961) 162.
15 A. Zlatkis and D. C. Fenimore, *Rev. Anal. Chem.*, 2, No. 4 (1975) 320.
16 E. W. McDaniel, *Collision Phenomena in Ionized Gases*, Wiley, New York, 1964, Appendix I, pp. 693–700.
17 I. Dzidic, D. I. Carroll, R. N. Stillwell and E. C. Horning, *Anal. Chem.*, 47 (1975) 1308.
18 E. C. Horning, D. I. Carroll, I. Dzidic, K. D. Haegele, M. G. Horning and R. N. Stillwell, *Anal. Chem.*, 12 (1974) 725.
19 M. McKeown and M. W. Siegel, *Amer. Lab.*, November (1975) 91.
20 C. A. Blank, M. H. Bortner, T. Baurer and A. A. Feryok, *A Pocket Manual of the Physical and Chemical Characteristics of the Earth's Atmosphere*, Defense Nuclear Agency, Washington, D.C. 20305, 1974, pp. 151–155.